Fracture 1977, Volume 2, ICF4, Waterloo, Canada, June 19 - 24, 1977

LOW CYCLE FATIGUE STRENGTH OF STEELS AND WELDS IN RELATION TO STATIC TENSILE PROPERTIES

K. Iida* and E. Fujii**

INTRODUCTION

The total strain amplitude ε_{Ta} in strain cycling fatigue consists of the plastic strain amplitude ε_{pa} and the elastic strain amplitude ε_{ea}. It is well known that both ε_{pa} and ε_{ea} are expressed by the so-called Manson-Coffin relation as $C_p . N^{-k_p}$ and $C_e . N^{-k_e}$ respectively, where C_p, C_e, k_p and k_e are material constants and N is the fatigue life. If we presume static tension as a limit of very low cycle fatigue, for instance a quarter cycle fatigue in case of reversed strain cycling, it may be naturally regarded that the static fracture ductility should be closely related with C_p and the tensile strength should be correlated with C_e.

From this point of view, and in addition in order to meet the demand of predicting low cycle fatigue strength from static tensile properties without carrying out fatigue tests, many researches have been made on the dependency of material constants in the above-mentioned power laws upon the tensile properties. A typical example of the results of such investigation is an equation derived by Manson [1] on the basis of strain cycling test results of 29 materials with wide variables in tensile strength, static fracture ductility and elastic modulus. In this equation of the failure life basis, that is called as universal slopes method, C_p and C_e are given as a function of static tensile properties: $C_p = \varepsilon_f^{0.6}/2$, $C_e = 1.75\sigma_u/E$, where ε_f, σ_u and E are static fracture ductility, tensile strength and Young's modulus, respectively. While k_p and k_e take constant values: 0.6 and 0.12 respectively.

Two points may be raised here for discussion about this equation. The first one is that all the accumulated data on strain cycling fatigue strength, which were used for the evaluation of the universal slopes method, were obtained for only base metals, although the low cycle fatigue behaviour of the weld metal may be considered one of the problems in the low cycle fatigue design of welded structures, in the light of the fact that the service failure of welded structures started frequently from the welds. The second one is that the derived equation by Manson is based on the failure life criterion.

The purpose of this paper is to find proper relations between the constants and tensile properties for a certain range of steels and weld metals by analyzing experimental data of the present results and previous test results on base metals. Another feature of the present work is the definition of the fatigue life with the criterion of the visible crack initiation life, which may be more realistic and practical criterion than the failure life in evaluating the low cycle fatigue strength data for the purpose of the fatigue design of a structure, because the fatigue life to the complete

* University of Tokyo, Hongo, Bunkyo-ku, Tokyo, Japan
** Ship Research Institute, Mitaka, Tokyo, Japan

MS220

separation of a specimen includes the crack propagation life that is an ambiguous value influenced by specimen size and the change of strain controlled conditions for the residual test section.

MATERIALS AND TESTING PROCEDURE

The steels used for testing, a mild steel and eight high strength steels, were received in the form of 19 to 100 mm thick rolled plate. After machining of one of three kinds of edge preparations shown in Figure 1, butt or groove welding was carried out by submerged arc welding in flat position. The welding was done with proper welding conditions to each steel except the test series No. 13 labelled HT-60-UJ, for which a filler wire for 490 MN/m^2 class high strength steel was applied for the welding of 588 MN/m^2 class steel with the intention of obtaining an under-matched joint.

The hour-glass shaped specimens of 1.06 in the theoretical stress concentration factor were cut out in the rolling direction at half plate depth from each base metal of as-received condition and from each butt welded joint as shown in Figure 1. Table 1 shows codes of the specimens, the diameter of the test section and tensile properties obtained with the hour-glass shaped specimen. The minimum cross section of the specimens of SM41-J (test series No. 6) and HT80-J (test series No. 8) was located at the point of the maximum hardness in the heat-affected-zone. The test section of the specimens of HT50-W, HT60-W and HT80-W (test series Nos. 10, 11 and 12) is fully the weld metal. In the test section of the specimens of HT60-UJ and HT60-NJ (test series Nos. 13 and 14), the sum of the girth length along the periphery of top and bottom weld metals is roughly equal to that along the periphery of the base metal. The static fracture as well as the low cycle fatigue crack started from the heat-affected-zone in SM41-J, HT80-J, HT60-UJ and HT60-NJ specimens.

Diametral natural strain amplitude was controlled under the condition of the reversed strain cycling (strain ratio = -1) in all the fatigue tests. More than nine specimens were tested for each test series at ambient temperature with the cycling rate of 1 to 60 cycles per minute.

RESULTS AND DISCUSSION

The plastic strain amplitude ε_{pa} and the elastic strain amplitude ε_{ea} in the longitudinal direction of a specimen are expressed with an assumption of uniform distributions of stress and strain through the test section as follows:

$$\varepsilon_{pa} = 2\varepsilon_{Ta}^{(d)} - \nu\sigma_R/E \;, \qquad \varepsilon_{ea} = \sigma_R/2E \tag{1}$$

where $\varepsilon_{Ta}^{(d)}$ is the diametral total strain amplitude, ν is Poisson's ratio and σ_R is the true stress range.

The ε_{pa} and ε_{ea} of a specimen in each test series were plotted in log-log scale against the visible crack initiation life N_c, that is the number of cycles to initiation of a crack 0.2 to 0.5 mm in length on surface of the test section. Thus the following equation was obtained by applying a power law to ε_{pa} versus N_c and ε_{ea} versus N_c curves respectively:

$$\varepsilon_{Ta} = C_p . N_c^{-k_p} + C_e . N_c^{-k_e} \tag{2}$$

where ε_{Ta} is the longitudinal total strain amplitude.

Possible correlations between these material constants and tensile properties were analyzed for the present results by putting together with reference data reported in previous papers [2 - 13], and then the followings were found.

(1) Constant C_p: In Figure 2 the constant C_p is plotted against the static fracture ductility ε_f. It is seen that the data scatters widely, but a median line may be derived by taking an increasing tendency of C_p into consideration.

$$C = 0.286\ \varepsilon_f \;. \tag{3}$$

(2) Exponent k_p: Figure 3 presents the relation between the exponent k_p and ε_f. The following equation may be derived from a slightly increasing dependency of k_p.

$$k_p = 0.0425\ \varepsilon_f + 0.544 \;. \tag{4}$$

(3) Constant C_e: The relation between the constant C_e and tensile strength is shown in Figure 4, which suggests the following equation.

$$C_e = 5.26 \times 10^{-6}\ \sigma_u + 0.0013 \qquad (\sigma_u \text{ in } MN/m^2) \;. \tag{5}$$

(4) Exponent k_e: The dependency of k_e upon the tensile strength is rather fair as shown in Figure 5, from which a median line is derived as follows:

$$k_e = -1.074 \times 10^{-4}\ \sigma_u + 0.173 \qquad (\sigma_u \text{ in } MN/m^2) \;. \tag{6}$$

The reason for the wide scatter bands observed in figures mentioned above may be explained by the sensitive change of constants and exponents in equation (2) in the application of a straight, median line fitting for a family of log-log plotted data of ε_{pa} versus N_c relation or ε_{ea} versus N_c relation. And the scatter of experimental results, that is proper to the fatigue test, will make the sensitive change increase too.

In Figure 6, the actual comparisons are made between the experiments and the predictions for each of 13 materials tested, excluding HT60(B) that has no data of ε_f. The ordinate stands for the ratio of an experimental ε_{Ta}, that is obtained at any N_c on the median line for the experimental results of ε_{Ta} versus N_c, to a predicted ε_{Ta}, that is obtained at the same N_c by applying equations (3), (4), (5) and (6). In most cases, the agreement is remarkably good in higher cycle range. Figure 6 also suggests that the predicting method proposed by the present paper will provide the prediction of low cycle fatigue strength within the accuracy range of ± 40 percent.

CONCLUSIONS

Completely reversed strain cycling fatigue tests were conducted on a certain range of high strength steels and weld metals. The material constants in Manson-Coffin equation of the visible crack initiation basis were examined in the relation to the tensile properties by referring previous data.

As a result of the present investigation, it can be concluded that the total strain amplitude in reversed strain cycling ε_{Ta} is predicted by the following formula within the accuracy range of ± 40 percent.

$$\varepsilon_{Ta} = 0.286\ \varepsilon_f \cdot N_c^{-(0.0425\varepsilon_f + 0.544)}$$

$$+ (5.26 \times 10^{-6}\ \sigma_u + 0.0013)\ .\ N_c^{-(0.173 - 1.074 \times 10^{-4}\sigma_u)}$$

where ε_f and σ_u are static fracture ductility ($= ln\ \frac{1}{1-RA}$, RA = reduction in area) and ultimate tensile strength in MN/m^2 respectively and N_c is visible crack initiation life.

REFERENCES

1. MANSON, S. S., Experimental Mechanics, 4, 1964, 193.
2. HOTTA, T., ISHIGURO, T., ISHII, N. and SEKIGUCHI, S., J. Soc. Naval Architects Japan, 128, 1970, 317.
3. IIDA, K., J. Soc. Naval Architects Japan, 119, 1966, 193.
4. IIDA, K., INOUE, H. and KOBAYASHI, Y., J. Soc. Naval Architects Japan, 121, 1967, 249 and 123, 1968, 287.
5. ANDO, Y., IIDA, K., SAKABE, K. and TSUKADA, H., IIW Doc. XIII-464-67, 1967.
6. ANDO, Y. and IIDA, K., Nuclear Engineering and Design, 8, 1968, 143.
7. IIDA, K., INOUE, H., KOBAYASHI, Y. and MIYAMOTO, T., J. Soc. Naval Architects Japan, 125, 1969, 217.
8. IIDA, K., FUKUDA, Y. and ANDO, Y., IIW Doc. XIII-534-69, 1969.
9. IIDA, K., First Int. Symposium of Japan Welding Society, Tokyo, 1971.
10. IIDA, K., Trans. Japan Welding Society, 2, 1971, 86.
11. IIDA, K., English Edition of J. Soc. Naval Architects Japan, 11, 1973, 117.
12. IIDA, K. and INOUE, H., J. Soc. Naval Architects Japan, 113, 1973, 235.
13. IIDA, K., MATSUMOTO, Y. and NAGAI, H., J. Soc. Naval Architects Japan, 137, 1975, 217.

Table 1 Test Series and Tensile Properties of Hour-Glass Type Specimen (Shape Factor = 1.06)

Test Series No.	Material Code	Material Kind [a]	Dia. of Specimen (mm)	Tensile Properties YP [b]	UTS [c]	RA [d]	ε_f [e]	Remarks [f]
1	A212B	B	10	328	590	58.0	0.868	
2	HT60(A)	B	5	579	685	70.1	1.207	
3	HT60(B)	B	12	496	674	-	-	
4	HT60(C)	B	7	535	685	59.0	0.892	
5	HT80(A)	B	10	862	901	63.4	1.005	
6	SM41-J	J	10	385	540	67.6	1.127	
8	HT80-J	J	10	715	849	53.1	0.757	
9	HT60(D)	B	7	464	599	72.6	1.295	
10	HT50-W	W	10	505	648	57.9	0.865	
11	HT60-W	W	10	524	662	55.6	0.812	
12	HT80-W	W	10	735	818	53.5	0.766	
13	HT60-UJ	P	10	532	631	58.4	0.877	U.M.
14	HT60-NJ	P	10	541	634	58.0	0.868	N.M.
16	HT80(C)	B	10	742	885	57.0	0.844	

[a] J: Butt Joint, W: Weld Metal, P: Parallel Type Welded Joint including Weld Metal, HAZ and Base Metal (All of the weld metal are deposited by sub-merged arc welding).
[b] Yield Stress in MN/m^2.
[c] Ultimate Tensile Strength in MN/m^2.
[d] Reduction in Area in percent.
[e] Static Fracture Ductility $\{= ln\ 100/(100 - RA)\}$.
[f] U.M. (Under Matched): Welding was done by using the filler wire for HT50 steel. N.M. (Normal Matched): Welding was done by using the filler wire for HT60 steel.

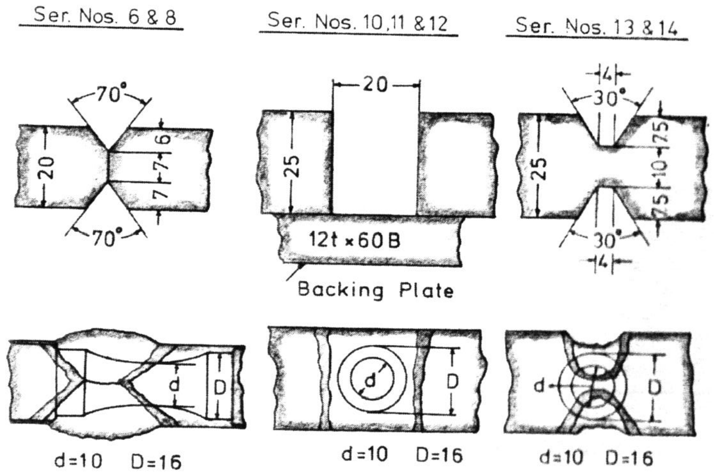

Figure 1 Edge Preparations and Locations of Test Specimen in Welded Joint

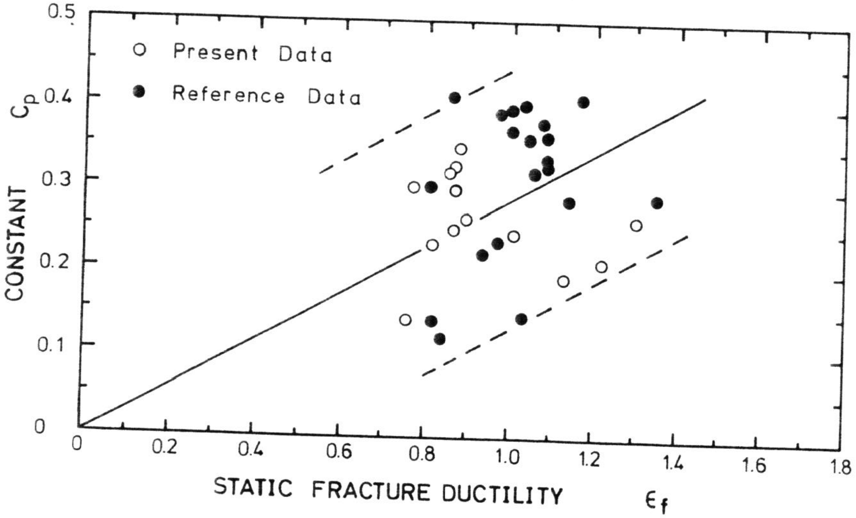

Figure 2 Relation Between C_p and ε_f

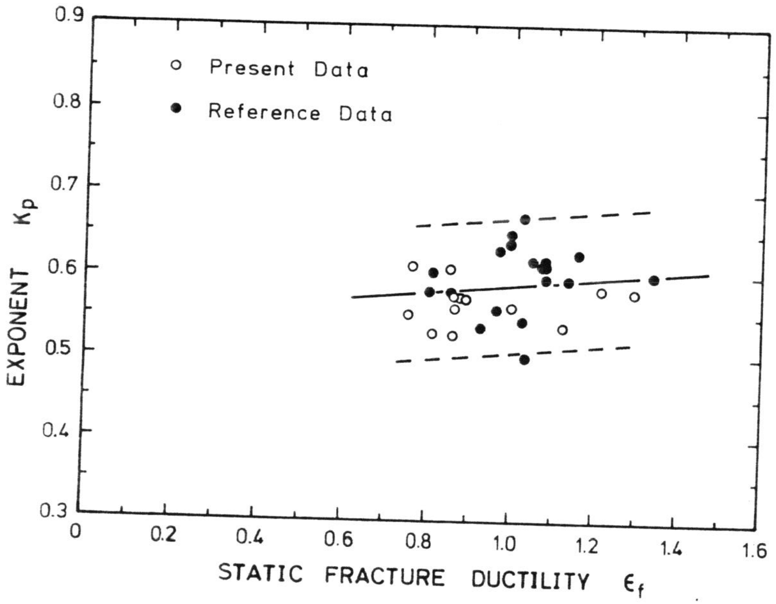

Figure 3 Relation Between k_p and ε_f

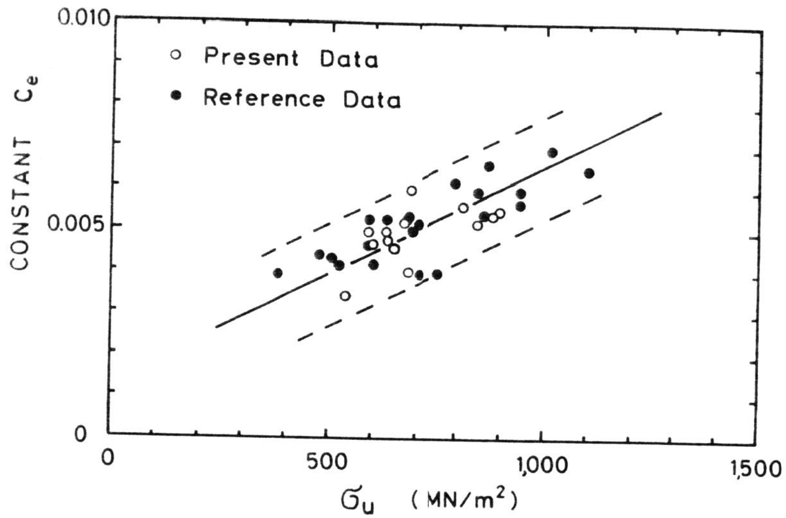

Figure 4 Relation Between C_e and σ_u

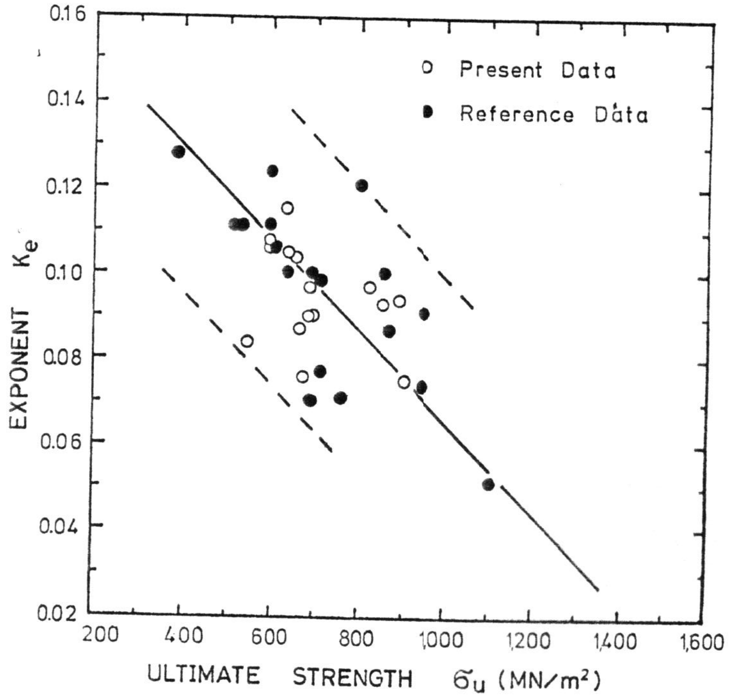

Figure 5 Relation Between k_e and σ_u

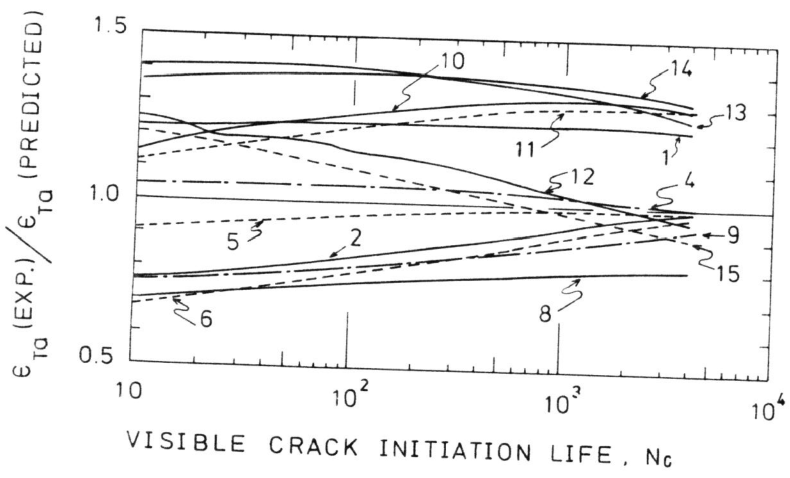

Figure 6 Ratio of Total Strain Amplitudes in Experiments and Predictions